Journal of Magnetic Resonance **156,** 19–25 (2002)
doi:10.1006/jmre.2002.2534

WAVEWAT—Improved Solvent Suppression in NMR Spectra Employing Wavelet Transforms

Ulrich L. Günther,[1] Christian Ludwig, and Heinz Rüterjans

Institute for Biophysical Chemistry, J.W. Goethe University, Frankfurt, Biocenter N230, Marie-Curie-Str. 9, 60439 Frankfurt, Germany

E-mail: ugunt@bpc.uni-frankfurt.de

Received August 20, 2001; revised March 5, 2002; published online May 31, 2002

WAVEWAT is a new processing algorithm to suppress the on-resonance water signal in NMR spectra. It is based on a multiresolution analysis (MRA) of the free induction decay (FID) using a dyadic discrete wavelet transform (DWT). The width of the suppressed signal can be adjusted so that signals close to water are recovered without distortion of the signal shape and intensity. Computational efficiency is comparable to that of convolution filters employing a Fourier transform.

INTRODUCTION

NMR spectra of biological or biochemical samples are frequently recorded in aqueous solution. The intensity of the water signal in the spectra of such samples is several orders of magnitude larger than the intensities of the signals originating from the sample. The suppression of the water signal has been a key issue for designing NMR spectrometers, experiments, and processing algorithms. Increased dynamic range of receivers combined with sophisticated strategies to suppress the water signal enable the detection of signals that have several orders of magnitude lower intensity than the water signal. Experimental techniques to minimize the signal of water include presaturation (*1*), nonexcitation using jump-return and binomial sequences (*2, 3*) spin-lock pulses in INEPT sequences (*4*), suppression of water employing pulsed field gradients combined with selective excitation (*5*), and heteronuclear experiments using the PEP-HSQC (*6*) pulse sequence. Although the intensity of the water resonance can be significantly reduced employing these techniques, the residual water signal is still larger and often broader than the signals of interest. A basic problem is the reconstruction of signals close to the water resonance. In the case of protein samples these are the signals of H^{α} protons which are important for the calculation of protein structures.

Several computational methods have been proposed to suppress the water resonance. Frequently, spectra are recorded with the water signal at zero frequency in the middle of the spectrum (on-resonance). A common method to suppress the water resonance is the subtraction of a low order polynomial which is fitted to the free induction decay (*7*). Marion *et al.* proposed a convolution filter in which the free induction decay (FID) is convoluted with a Gaussian or sine bell window (*8*). Subtraction of the convoluted signal eliminates the on-resonance component of the signal. A fast algorithm to calculate the convolution using fast Fourier transformations was later proposed by Craven *et al.* (*9*). Other alternatives include the use of Gabor transforms and continuous wavelet transforms (CWT) (*10–12*). Five different filtering approaches including the Gabor transformation (*10*), the convolution method (*8*), a filtering method of Sodano and Delepierre (*13*), a highpass butterworth filter described by Cross (*14*), and a recently described finite impulse response filter (*15*) were compared in a recent review (*16*). The water resonance can also be eliminated by employing a singular value decomposition (SVD) (*17, 18*) on a Hankel-type matrix derived from the FID and suppression of the largest singular value(s). After reconstruction of the FID the largest signals are eliminated. Although this algorithm is very powerful it is not feasible for large spectra because the SVD is computationally very demanding. In addition, SVD-based water suppression may influence the intensity of other signals in the spectrum.

Water suppression algorithms must satisfy several criteria: First, the water signal should be suppressed efficiently; second, signals close to water should be recovered; and third, water suppression should not cause any distortions in other regions of the spectrum. Here we propose a new method based on discrete wavelet transforms (DWT) applied to time domain data to suppress the on-resonance water signal. It will be shown that efficient water suppression can be achieved and signals close to water can be recovered without distortion.

EXPERIMENTAL

WAVEWAT and other processing routines employed in this work were implemented within the MATLAB (The Mathworks) integrated development environment. Spectra were processed using the NMRLAB processing package (*19*). Fast wavelet transforms were calculated employing routines from WAVELAB (*20*).

[1] To whom correspondence should be addressed.

1090-7807/02 $35.00

Wavelet transformation will here only be introduced briefly because the principles of wavelet transforms are summarized in several excellent textbooks (*21, 22*). Two different types of wavelet transformation are commonly used in signal processing: *continuous* wavelet transformation and *discrete* wavelet transformation. Continuous wavelet transformation was previously used to suppress the solvent signal (*12*). Here we used a discrete wavelet transform for multiresolution analysis (MRA). DWT requires a basis set of orthonormal wavelets which are derived from a mother wavelet by *dyadic dilatations* and integer *translations*. With j denoting the dilatation index and k representing the translation index a family of wavelets can be derived from a mother wavelet ψ according to

$$\psi_{j,k}(x) = 2^{j/2}\,\psi(2^j x - k) \qquad [1]$$

for integer values j and k. The mother wavelet must have compact support, i.e., $\psi = 0$ outside a finite interval. The $2^{j/2}$ is a scaling factor which arises from the normalization condition

$$\int_{-\infty}^{\infty} \psi_{j,k}^2 = 1. \qquad [2]$$

Since the wavelet is scaled and shifted the WT yields a time-frequency representation of the signal.

A simple wavelet which is often used to explain the principles of the wavelet transform is the Haar wavelet:

$$\psi_{\text{Haar}} = \begin{cases} 1, & 0 \le x < \dfrac{1}{2} \\ -1, & \dfrac{1}{2} \le x < 1 \\ 0, & \text{otherwise.} \end{cases} \qquad [3]$$

For the Haar wavelet ψ the derived wavelets $\psi_{j,k}$ also have a compact support

$$\text{supp}(\psi_{j,k}) = [k2^{-j}, (k+1)2^{-j}). \qquad [4]$$

Now any square integrable function[2] $f(x)$ can be described by

$$f(x) = c_{00}\phi(x) + \sum_{j=0}^{n-1}\sum_{k=0}^{2^j-1} c_{j,k}\psi_{j,k}(x), \qquad [5]$$

where $c_{j,k}$ are wavelet coefficients, $\psi_{j,k}$ are wavelets derived from a mother wavelet ψ, and ϕ is a scaling function (father wavelet); in the case of the Haar wavelet transform it is unity on the interval [0, 1). Using Eq. [5] a function f can be decomposed into a linear combination of wavelets $\psi_{j,k}$. The same is true for a data series which can be described by a function $f(x)$.

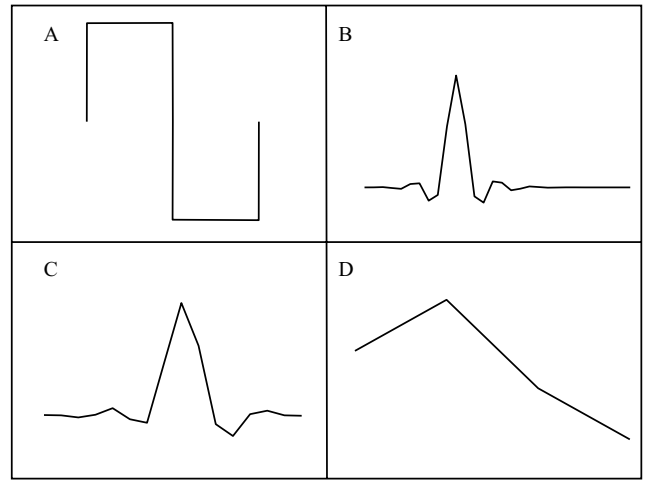

FIG. 1. Typically used wavelets. (A) Haar, (B) Coiflet (5), (C) Symmlet (8), (D) Daubechies (5) wavelet. The numbers in parentheses describe the wavelet parameter.

Commonly used wavelets are more complex than the Haar wavelet which is not very efficient to approximate smooth functions. More complex wavelets require a smaller number of wavelet coefficients $c_{j,k}$ to compose a signal. Typical wavelets used for water suppression are shown in Fig. 1 (*23, 24*). Fast algorithms are available to calculate wavelet coefficients (*21, 22, 25*). A brief introduction to the process of calculating the wavelet coefficients can be found in the Appendix.

MRA was introduced by Mallat (*22, 26*). It is based on the idea that a function $f(x)$ can be approximated at different dilatation levels j. Each approximation f_j can be written as an approximation on a coarser level f_{j-1} and a detail function. The higher the level j the finer the approximation f_j of the original function and the lower the level j the coarser the approximation. Thus j describes the resolution level of the function approximation. For the formal definition of MRA which requires the introduction of a ladder of nested subspaces for the different resolution levels j we refer to the previously mentioned textbooks on wavelets (*21, 22*). It is important to note that the dyadic scaling of wavelets $\psi_{j,k}$ used in MRA limits the number of resolution levels to $J = 2^N$ where N is the number of data points.

RESULTS

MRA is a useful tool to decompose a signal into time-scale components. In the case of time domain NMR data this corresponds to a decomposition in different frequency ranges. This is demonstrated in Fig. 2 which depicts a multiscale plot of an experimental FID originating from a ^{15}N-HSQC spectrum of an SH2 domain. This plot was calculated by transforming back signal components at different dyadic levels. The sum of the signals

[2] For square integrable functions $\|f\| = (\int_{\infty}^{\infty} f^2(x)\,dx)^{1/2} < \infty$ for $x \in \mathbb{R}$, i.e., $f \in \mathbb{L}^2(\mathbb{R})$. $\mathbb{L}^2(\mathbb{R})$ is a Banach space of square integrable functions.

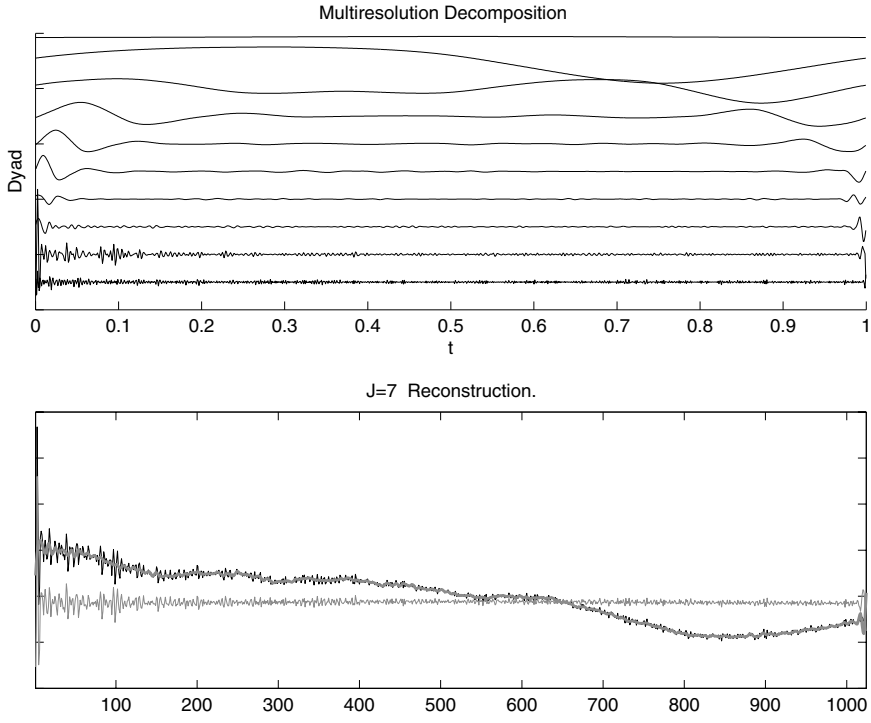

FIG. 2. Top, multiresolution plot of a FID from a ^{15}N-HSQC spectrum recorded at 500 MHz using a 1.2-mM protein sample. Bottom, original FID and FID recovered from the MRA (gray) shown in Fig. 1 only using levels with $J \geq 7$.

at all dyadic levels is equivalent to the original signal. Leaving out levels corresponding to low numbers of j will eliminate low frequency components of the signal. A basic limitation is the fact that the number of dyadic levels is limited by $2^J = N$ because the number of dyadic levels determines the width of the filter. A sufficiently large number of data points for a reasonably narrow filter width was obtained by repeated zero filling of the FID. Another problem arose from edge effects, particularly at the end of the FID where the signal intensity is low as can be seen in Fig. 2. Edge effects could be eliminated by adding a mirror image of the FID on the negative time axis.

The filter characteristics of WAVEWAT are illustrated in Fig. 3 employing a test spectrum which consists of a series of equally spaced lines with a separation of 25 Hz. The dwell time was set to 125 μs equivalent to a 8000-Hz sweep width. Figure 3A depicts the central part of this test spectrum. Figure 3B shows the result after applying a 64-point convolution filter to the time domain signal followed by Fourier transformation. For this combination of dwell time and width of the Gaussian convolution filter a broad range of approximately 400 Hz is affected. The width of the distortion can be significantly reduced by increasing the number of points of the convolution function. This is demonstrated in Fig. 3C using a 128-point Gaussian convolution function. It should be emphasized that the width of the convolution window increases with the dwell time of the spectrum and is in principle independent of the number of data points. However, the size of the convolution window must be significantly smaller than

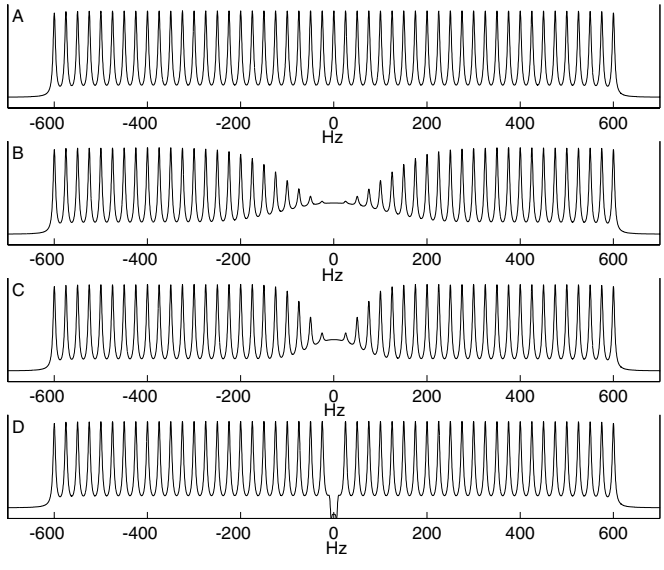

FIG. 3. (A) Synthetic test spectrum sampled in the time domain using a dwell time between data points of 125 μs (corresponding to a sweep width of 8000 Hz) with peaks separated by 25 Hz. The shown test spectrum was obtained after applying a fast Fourier transform to the corresponding free induction decay. (B) Test spectrum from (A) after applying a 64-point convolution filter to the corresponding signal in the time domain followed by Fourier transform. (C) Test spectrum from (A) after applying a 128-point convolution filter to the corresponding signal in the time domain followed by Fourier transform. (D) Test spectrum from (A) after applying WAVEWAT suppressing 7 dyadic levels using a symmlet-8 wavelet and mirror reflection of the FID.

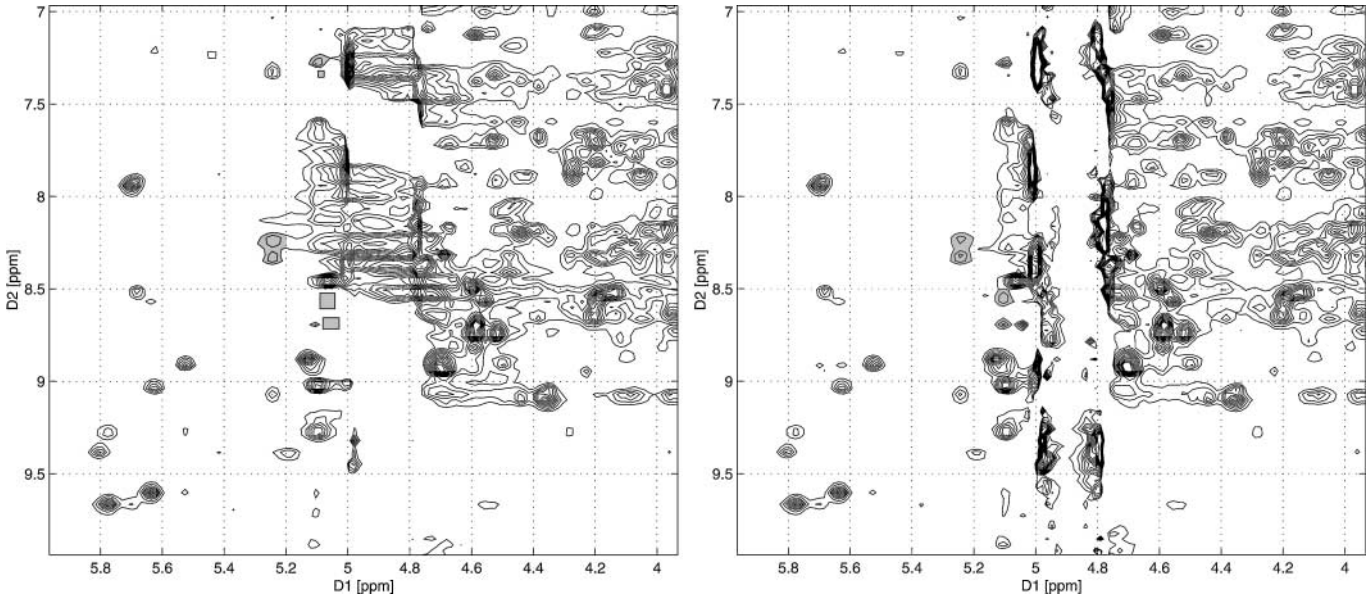

FIG. 4. NOESY spectrum of flavodoxin *desulfovibrio vulgaris* recorded at 500-MHz proton frequency with presaturation applied during recycle delays. Left, the water resonance was suppressed using a Gaussian convolution filter using 128 points for the filter. Right, the water resonance was suppressed using WAVEWAT with a Daubechies 20 wavelet (4-fold zero-filling using 6 dyadic levels for the reconstruction).

the number of data points in the FID. Figure 3D depicts filter characteristics of WAVEWAT eliminating 7 dyadic levels using a symmlet-8 as a wavelet and mirror reflection of the FID. This figure shows the sharpness of the edge of the WAVEWAT filter. The central signal is suppressed without any distortion of other signals.

Figure 4 compares 2D-NOESY spectrum of flavodoxin *desulfovibrio vulgaris* processed with a 128-point Gaussian convolution filter and with WAVEWAT (using a Daubechies 20 wavelet, fourfold zero-filling, and 6 dyadic levels for the restoration of the FID). In both spectra the filter parameters were chosen to suppress a sufficiently narrow region around the water signal to observe peaks close to the water resonance. In both cases some residual water signal is observed. In Fig. 4A some of the differences between both peaks are marked gray. The sharper edges of the WAVEWAT filter allow the detection of a few extra signals and avoid distortions on the edge of the filter.

DISCUSSION

Water suppression is an important step in processing NMR spectra of biological samples. This includes NMR spectroscopy of biomolecules as well as *in vivo* spectroscopy. Despite many efforts to reduce the contribution of the water signal to the overall FID the signal with the highest intensity is still often the water signal. Because the width of the water resonance at the maximum intensity of signals of the sample is usually significantly higher than the width of signals of the sample it is desirable to suppress the water signal in the time domain. The choice of the technique used to suppress the water resonance depends on the type of the spectrum. SVD based water suppression is powerful for *in vivo* spectra with relatively few data points but impractical for high resolution spectra with a large number of data points or multidimensional spectra with a large number of FIDs. The most commonly used techniques are polynomial subtraction and the subtraction of convolutions of the signal with functions with a compact support. Polynomial subtraction does not completely eliminate the water signal and convolution based water suppression distorts signal intensities close to the water signal. For this reason there has been continuous interest in other more powerful techniques to solve the problem. The technique presented here combines a number of powerful properties: It affects only a narrow region of the spectrum and is computationally very efficient.

WAVEWAT water suppression depends on few adjustable parameters: First, the type of wavelet must be chosen. Daubechies, coiflet, and symmlet wavelets proved to be almost equally suitable. Second, if the number of data points is smaller then 512, zero-filling the FID has been useful to tune the width of the suppression filter. Third, the user can choose the number of levels to be suppressed according to the desired bandwidth of signal removal. It should be noted, however, that off-resonance solvent signals can be suppressed after phase shifting complex time domain data points.

Computational efficiency. The proposed method performs comparably to the convolution method originally proposed by Marion *et al.* (*8, 9, 27*) if the latter is calculated employing a fast Fourier transform according to the convolution theorem

$$\mathfrak{F}\{S(t) \star g(t)\} = \mathfrak{F}\{S(t)\} \cdot \mathfrak{F}\{g(t)\},$$

where $S(t)$ represents the signal and $g(t)$ the convolution function (e.g., a Gaussian function). The convolution filter requires approximately $2N\log(N)$ operations (if g is short compared to S, its Fourier transform is calculated comparably fast). The DWT-filter proposed here must calculate a forward (FWT) and an inverse wavelet transform (IWT) which requires $2N$ operations. When zero-filling is used to reduce the width of the filter by increasing the number of dyadic levels computational efficiency suffers from an increased number of points N which must be transformed. In our experience 1024 or 2048 points (2^{10} and 2^{11}) are appropriate.

In summary, WAVEWAT is a highly efficient algorithm based on discrete wavelet transforms. It is suitable for large data sets and allows recovery of signals close to that of the solvent. Further applications of the technique include reconstruction of the FID using only low order levels representing the water signal. This allows the calculation of the area under the water signal which is often required in *in vivo* spectroscopy.

APPENDIX

A comprehensive description of the principles of wavelet transforms, construction of wavelets, and algorithms is far beyond the scope of this work. An in-depth derivation of the theory is found in (*21, 22, 25*). Here we will briefly describe the very basic principles of the dyadic discrete wavelet transform.

Let $f[n]$ be a time signal which is uniformly sampled at intervals t_{dw}. Let the size of the discrete signal be N. The discrete dyadic wavelet transformation (DWT) can be derived from the continuous formula

$$\mathcal{W}f(u,s) = \langle f, \psi_{u,s}\rangle = \int_{-\infty}^{\infty} f(t)\frac{1}{\sqrt{s}}\psi^*\left(\frac{t-u}{s}\right)dt$$

by using a discretized wavelet with compact support

$$\psi_j[n] = \frac{1}{\sqrt{2^j}}\psi\left(\frac{n}{2^j}\right).$$

The star in the above formula denotes the complex conjugation. The DWT is computed at different scales $s = 2^j$ using recursive application of low- and highpass filters, expressed as linear transformations as

$$\mathcal{L}^N f[n] = \sum_l h_l f[(l+2n) \bmod N]$$

$$\mathcal{H}^N f[n] = \sum_l \lambda_l f[(l+2n) \bmod N],$$

where n ranges from 0 to $N/2-1$.

The DWT is now performed by iterated application of these filters. Start with the entire data vector consisting of $N = 2^K$ entries. The following two vectors are then recursively computed by the DWT,

$$\{\alpha(j,k), k = 0,\ldots,2^j-1\}, \qquad \{\beta(j,k), k = 0,\ldots,2^j-1\}$$

with $0 \le j \le K-1$. The α's and β's are the lowpass and highpass filtered signals, respectively:

$$\alpha(j,k) = \mathcal{L}^{2j+1}\alpha(j+1,k)$$
$$\beta(j,k) = \mathcal{H}^{2j+1}\beta(j+1,k).$$

The $\alpha(j,k)$ and $\beta(j,k)$ approximate the exact wavelet coefficients, which are given by

$$\alpha_{j,k} = \langle f, \phi_{j,k}\rangle = \sum_l h_{l-2k}\alpha_{j+1,l}$$

$$\beta_{j,k} = \langle f, \psi_{j,k}\rangle = \sum_l \lambda_{l-2k}\alpha_{j+1,l}$$

with $\lambda_k = (-1)^{k+1}h_{1-k}$ and h_k are the coefficients of $m_0(\xi)$:

$$m_0(\xi) = \frac{1}{\sqrt{2}}\sum_k h_k \exp(-ik\xi).$$

$\phi_{j,k}$ is the father and $\psi_{j,k}$ the corresponding mother wavelet.

The different coefficients h_l correspond to the wavelet used to perform the DWT. The calculation of those coefficients may be described using an approach where wavelets are understood as a hierarchical filter bank (*28*). Suppose a filter B that is zero for "smooth" signals, e.g., that is, vanishing for a constant signal and for a linear ramp:

$$b_0\cdot 1 + b_1\cdot 1 + b_2\cdot 1 + b_3\cdot 1 = 0$$
$$b_0\cdot 0 + b_1\cdot 1 + b_2\cdot 2 + b_3\cdot 3 = 0.$$

Suppose another filter C, which does exactly the opposite. This results in

$$c_0b_0 + c_1b_1 + c_2b_2 + c_3b_3 = 0$$

because the C filter has vanishing coefficients when the B filter does not and *vice versa*. A pair of such filters is called *quadrature mirror filters*. A possible solution for this equation is

$$b_0 = c_3, \qquad b_1 = -c_2, \qquad b_2 = c_1, \qquad b_3 = -c_0,$$

resulting in

$$-c_0 + c_1 - c_2 + c_3 = 0$$

and

$$-3c_0 + 2c_1 - c_2 = 0$$

for the two filter conditions for the constant and the linear ramp of the input signal. We require further that the transformation with these filters has to be orthogonal, resulting in two additional nontrivial equations:

$$c_0^2 + c_1^2 + c_2^2 + c_3^2 = 1$$

and

$$c_0 c_2 + c_1 c_3 = 0.$$

We have now four equations with four unknowns, which have the solution

$$c_0 = \frac{1+\sqrt{3}}{4\sqrt{2}}, \qquad c_1 = \frac{3+\sqrt{3}}{4\sqrt{2}}$$

$$c_2 = \frac{3-\sqrt{3}}{4\sqrt{2}}, \qquad c_1 = \frac{1-\sqrt{3}}{4\sqrt{2}}.$$

The coefficients calculated so far are known as those for a Daubechies-4 wavelet.

Supplementary Material

All sources for the WAVEWAT algorithm are available on the Internet. Routines listed in the following table (and subroutines called from these routines) are required:

Programs from Wavelab and from NMRLab(http://www.nmrlab.net). Used for Wavelab (http://www.stat.stanford.edu/~wavelab)

Rewavelab	FWT_PO	Forward Wavelet Transform (periodized, orthogonal)
	IWT_PO	IWT_PO – Inverse Wavelet Transform (periodized, orthogonal)
nmrlab	WAVEWAT	Eliminate on-resonace signal from an FID by MRA

Program Sources for Fig. 2

The following script will reproduce Figs. 2A–2D. The execution of this script in MATLAB requires that NMRLab and WAVELAB be installed.

```
fid = ifft(ifftshift(SPC));
fid_lr = fid(1:1024*2);
clear fid FID
FID = fid_lr;
clear SPC
SPC = fftshift(fft(FID));
TD = length(FID);
clear xaxis
xaxis=linspace(-SWH/2,SWH/2,TD);
subplot(4,1,1)
plot(xaxis,real(SPC))
set(gca,'XLim',[-700,700],'YLIM',[-20,420],'YTick',[],
  'FontSize',12)
text(-690,370,'A','FontSize',12)
xlabel('Hz','FontSize',12)
% ******************************
fid_cnv_hr_1 = sol(FID,par1,par2);
spc_cnv_hr_1 = fftshift((fft(fid_cnv_hr_1)));
subplot(4,1,2)
plot(xaxis,real(spc_cnv_hr_1)) set(gca,'XLim',[-700,700],
  'YLIM', [-20,420],'YTick',[],'FontSize',12)
text(-690,370,'B','FontSize',12) xlabel('Hz','FontSize',12)
% ******************************
par1 = 64
par2 = 32
fid_cnv_hr_2 = sol(FID,par1,par2);
spc_cnv_hr_2 = fftshift((fft(fid_cnv_hr_2)));
subplot(4,1,3)
plot(xaxis,real(spc_cnv_hr_2)) set(gca,'XLim',[-700,700],
  'YLIM', [-20,420],'YTick',[],'FontSize',12)
text(-690,370,'C','FontSize',12)
xlabel('Hz','FontSize',12)
% ******************************
fid_ww = wavewat(FID,1,7,'Symmlet',8,1);
spc_ww = fftshift((fft(fid_ww)));
subplot(4,1,4)
plot(xaxis,real(spc_ww)) set(gca,'XLim',[-700,700],'YLIM',
  [-20,420],'YTick',[],'FontSize',12)
text(-690,370,'D','FontSize',12)
xlabel('Hz','FontSize',12)
```

ACKNOWLEDGMENTS

This work was supported by the RTD project FIND from the European community. We thank F. Löhr for providing a NOESY spectrum of his favorite protein which was recorded at the Frankfurt University Center for Biomolecular NMR.

REFERENCES

1. G. Wider, R. Hosur, and K. Wüthrich, Suppression of the solvent resonance in 2D NMR spectra of proteins in H_2O solution, *J. Magn. Reson.* **52,** 130–135 (1983).
2. P. Plateau and M. Gueron, Exchangeable proton NMR without base-line distorsion, using new strong-pulse sequences, *J. Am. Chem. Soc.* **104,** 7310–7311 (1982).
3. P. Hore, Solvent suppression in Fourier transform NMR, *J. Magn. Reson.* **55,** 283–300 (1983).
4. B. A. Messerle, G. Wider, G. Otting, C. Weber, and K. Wüthrich, Solvent suppression using a spin lock in 2D and 3D NMR spectroscopy with aqueous solutions, *J. Magn. Reson.* **85,** 608–613 (1989).
5. M. Piotto, V. Saudek, and V. Sklenar, Gradient-tailored excitation for single-quantum NMR spectroscopy of aqueous solutions, *J. Biomol. NMR* **2,** 661–666 (1992).
6. J. Cavanagh and M. Rance, Sensitivity enhanced NMR techniques for the study of biomolecules, *Annu. Rep. NMR Spectrosc.* **27,** 1–58 (1993).
7. A. Bielecki and M. Levitt, Frequency-selective double-quantum-filtered COSY in water, *J. Magn. Reson.* **82,** 562–570 (1989).

8. A. D. Marion, Improved solvent suppression in one- and two-dimensional NMR spectra by convolution of time-domain data, *J. Magn. Reson.* **84,** 425–430 (1989).
9. C. Craven and J. Waltho, The action of time-domain convolution filters for solvent suppression, *J. Magn. Reson. B* **106,** 40–46 (1995).
10. D. Barache, J. Antoine, and J. Dereppe, The continuous wavelet transform, an analysis tool for NMR spectroscopy, *J. Magn. Reson.* **128,** 1–11 (1997).
11. J. Antoine, A. Coron, and J. Dereppe, Water peak suppression: Time-frequency vs time-scale approach, *J. Magn. Reson.* **144,** 189–194 (2000).
12. H. Serraï, L. Senhadji, J. DeCertaines, and J. Coatrieux, Time-domain quantification of amplitude, chemical shift, apparent relaxation time t_2^* and phase by wavelet-transform analysis: Application to biomedical magnetic resonance spectroscopy, *J. Magn. Reson.* **124,** 20–34 (1997).
13. P. Sodano and M. Delepierre, Clean and efficient suppression of the water signal in multidimension NMR spectra, *J. Magn. Reson. A* **104,** 88–92 (1993).
14. K. Cross, Improved digital filtering technique for solvent suppression, *J. Magn. Reson. A* **101,** 220–224 (1993).
15. T. Sundin, L. Vanhamme, P. Van Hecke, I. Dologlou, and S. Van Huffel, Accurate quantification of 1 H spectra: From finite impulse response filter design for solvent suppression to parameter estimation, *J. Magn. Reson.* **139,** 189–204 (1999).
16. A. Coron, L. Vanhamme, J.-P. Antoine, P. Van Hecke, and S. Van Huffel, The filtering approach to solvent peak suppression in MRS: A critical review, *J. Magn. Reson.* **152** (2001).
17. W. Pijnappel, A. van den Boogaart, R. de Beer, and D. van Ormondt, SVD-based quantification of magnetic resonance signals, *J. Magn. Reson.* **97,** 122–134 (1992).
18. G. Zhu, D. Smith, and Y. Hua, Post-acquisition solvent suppression by singular-value decomposition, *J. Magn. Reson.* **124,** 286–289 (1997).
19. U. Günther, C. Ludwig, and H. Rüterjans, NMRLAB—Advanced NMR data processing in Matlab, *J. Magn. Reson.* **145,** 101–108 (2000).
20. J. Buckheit and D. Donoho, Wavelab and reproducible research, *in* "Wavelets and Statistics" (A. Antoniadis and G. Oppenheim, Eds.), pp. 53–81, Springer-Verlag, Berlin (1995).
21. I. Daubechies, "Ten Lectures on Wavelets," SIAM, Philadelphia (1992).
22. S. Mallat, "A Wavelet Tour of Signal Processing," Academic Press, San Diego (1998).
23. I. Daubechies, Orthonormal bases of compactly supported wavelets, *Commun. Pure Appl. Math.* **41,** 909–996 (1988).
24. A. Oppenheim and R. Schaefer, "Discrete-Time Signal Processing," Prentice-Hall, Englewood Cliffs, NJ (1989).
25. W. Härdle, G. Kerkyacharian, D. Picard, and A. Tsybokov, Wavelets, approximation, and statistical applications, *in* Lecture Notes in Statistics, Springer-Verlag, New York/Berlin (1998).
26. S. Mallat, Multiresolution approximations and wavelet orthonormal bases of $L^2(R)$, *Trans. Amer. Math. Soc.* **315,** 69–87 (1989).
27. W. Press, S. Teukolsky, and W. Vetterling, "Numerical Recipes in C: The Art of Scientific Computing," Cambridge Univ. Press, Cambridge, UK (1992).
28. N. Gershenfeld, "The Nature of Mathematical Modeling," Cambridge Univ. Press, Cambridge, UK (1999).